CARBON 50 (2012) 5286–5291

Available at www.sciencedirect.com

SciVerse ScienceDirect

journal homepage: www.elsevier.com/locate/carbon

The doping of reduced graphene oxide with nitrogen and its effect on the quenching of the material's photoluminescence

Ming Li [a,c], *Zhongshuai Wu* [b], *Wencai Ren* [b], *Huiming Cheng* [b], *Nujiang Tang* [a,*], *Wenbin Wu* [a], *Wei Zhong* [a], *Youwei Du* [a]

[a] *Physics Department, Nanjing National Laboratory of Microstructures, Nanjing University, Nanjing 210093, PR China*
[b] *Shenyang National Laboratory for Materials Science, Institute of Metal Research, Chinese Academy of Sciences, Shenyang 110016, PR China*
[c] *College of Science, Guilin University of Technology, Guilin 541004, PR China*

ARTICLE INFO

Article history:
Received 11 May 2012
Accepted 7 July 2012
Available online 16 July 2012

ABSTRACT

N-doped graphene (NG) was synthesized by annealing reduced graphene oxide (RGO) in an ammonia atmosphere. The dependence of the nitrogen content on the annealing temperature and the type of doping of NG were investigated. The photoluminescence (PL) properties of the RGO and NG samples were studied. The results show that RGO exhibits strong ultraviolet (UV) PL at 367 nm. The PL of RGO can be quenched by doping it with N and the quenching efficiency depends on the pyridine N content.

1. Introduction

Graphene, a two-dimensional single atomic layer of hexagraphenenal carbon network, has aroused special attention since it was isolated by Geim et al. in 2004 [1]. Recent reports showed that graphene dispersions have a significant optical response to nanosecond laser pulses at 532 and 1064 nm [2], and functionalization of graphene can alter its electronic structure resulting in interesting electronic and optical properties. Moreover, graphene oxide (GO) has interesting nonlinear absorption in dimethylformamide and a large two-photon absorption coefficient [3].

Furthermore, fluorescence quenching has been widely used in the selective detection of biomolecules, resonance Raman spectroscopy, etc. [4–6]. For example, fluorescence quenching of porphyrin by graphene and photophysical properties of porphyrin-graphene complexes have been reported [7,8]. Wherein, it is believed that electron or energy transfer between graphene and the aromatic molecule would be responsible for the phenomenon. Matte et al. reported the quenching of fluorescence of two aromatic molecules by non-covalent interaction with graphene, and demonstrated the occurrence of intermolecular photo-induced electron transfer [9]. More recently, Bi et al. confirmed that GO can highly adsorb single-stranded DNA, resulting in effectively quenching the emission of organic dyes [10]. Theaterical studies also confirmed that long-range energy transfer is effective in the fluorescence quenching of electron donor molecule in the presence of graphene [11,12].

Notably, many efforts have been devoted to investigating N-doped graphene (NG) because doping graphene with N could be a promising route to improve its electronic and optical properties for various applications. For example, n-type semiconductor can be obtained by substituting carbon atoms with nitrogen atoms in graphene frameworks [13,14]. Theoretically, the substitutional heteroatom doping can tune the band structure of graphene, resulting in a metal-semiconductor transition, thus expanding the applications of graphene [15,16]. Up to now, almost all experimental and theaterical works have focused on their electronic and thermal properties.

* *Corresponding author.*
E-mail address: tangnujiang@nju.edu.cn (N. Tang).
0008-6223/$ - see front matter
http://dx.doi.org/10.1016/j.carbon.2012.07.015

However, little work has been done on the optical properties of NG. In this paper, NG samples were synthesized by annealing RGO in an ammonia atmosphere, and the dependence of the nitrogen content on annealing temperature and the type of doping of NG were studied. Moreover, the photoluminescence (PL) properties of NG at room temperature (RT) were also investigated. The results showed that RGO exhibits strong ultraviolet (UV) PL at 367 nm. Interestingly, by doping it with N, the PL intensity of RGO can be quenched and the quenching efficiency is closely related to pyridine N content.

2. Experimental

The RGO sheets were synthesized by chemical exfoliation of natural flake graphite powder (500 mesh) followed by thermal reduction, as reported previously [17,18]. The NG samples (NG-300, NG-500, NG-700, and NG-800, numeric numbers denote the annealing temperature) were prepared from 300 to 800 °C for 1 h under an ammonia atmosphere. In short, a flow of Ar gas (99.99%) with a flow rate of 100 sccm was maintained to get rid of air for 20 min. After heating from RT to the desired temperature, the ammonia was introduced into the reaction tube with the flow rate of 20 sccm for 1 h at atmospheric pressure. After the furnace cooled to RT, the NG sample was obtained.

The morphologies of the samples were examined by transmission electron microscopy (TEM) (Model JEOL-2010, Japan) operated at an accelerating voltage of 120 kV. X-ray photoemission spectroscopy (XPS) measurements were performed on a Thermo Fisher Scientific with Al Kα radiation. The Raman spectra were obtained by an InVia Raman system (Renishaw, England) using 514.5 nm laser as the light source. The PL spectra were measured at ambient conditions by a spectrofluorophotometer (Shimadzu RF-5301PC) using a Xe lamp as the light source. For PL spectra investigation, ~0.03 mg of powdered sample was ultrasonically dispersed in 1 mL of distilled water for 0.5 h. After that, the solution was used.

3. Results and discussion

Fig. 1 shows the typical TEM images of the RGO and NG-500. As can be seen from Fig. 1, NG-500 still maintains the two dimensional ultrathin flexible structure, but has more corrugations and scrolling than RGO.

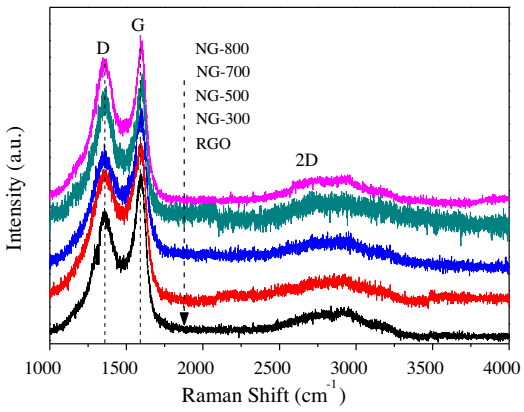

Fig. 2 – Raman spectra of the RGO and NG samples obtained at different annealing temperatures.

Shown in Fig. 2 are the Raman spectra of the RGO and NG samples obtained at different annealing temperatures. All the Raman spectra exhibit two prominent peaks of the D band and G band as well as a very weak 2D band, which is typical characteristic of chemically derived graphene [19–21]. It is known that the D band is disordered band associated with structural defects and partially disordered structures of the sp^2 domains, while G band corresponds to the first-order scattering of the stretching vibration mode E_{2g} observed for sp^2 carbon domains. Generally, the intensity ratio of D band to G band (I_D/I_G) is used to estimate the disorder of graphene [21,22]. One can find that all the NG samples show higher I_D/I_G (0.92–0.98) than RGO (0.81). This indicates that the NG samples are more disordered than the RGO, which is consistent with the corrugation and scrolling structure observed by TEM investigations above. Moreover, similar to the N-doped graphitic materials reported [19,22–24], the shift of G band is due to the structural distortion of RGO caused by the different bond distances of C–C and C–N. Thus, the larger I_D/I_G and upshift of the G band observed for NG samples may suggest the N doping in RGO. One can calculate the in-plane graphite crystallite sizes (La) of the RGO and NG samples based on Raman data by the formula [25]

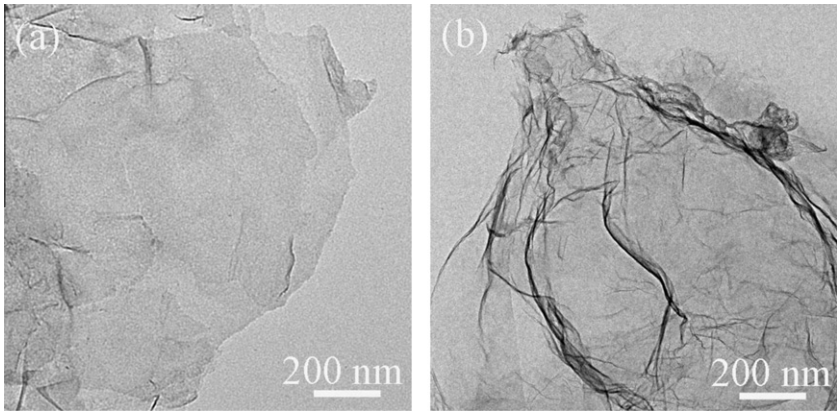

Fig. 1 – Typical TEM images of (a) RGO and (b) NG-500.

$$La\ (nm) = (2.4 \times 10^{-10})\lambda^4 (I_D/I_G)^{-1}$$

Where λ is the wavelength used for Raman measurements, while I_D and I_G denote the intensity of the D band and G band, respectively. The crystallite sizes of the RGO, NG-300, NG-500, NG-700, and NG-800 samples are estimated to be 20.8, 18.3, 18.1, 17.2, and 17.5 nm, respectively. Clearly, the NG samples show smaller crystallite sizes compared to RGO.

To detect the nitrogen content and bonding environment of the C and N species of NG samples, XPS measurements were employed. As shown in Fig. 3(a), the XPS spectra reveal that the clear N signals exist in all the NG samples. The N contents defined as 100 N/(C + N + O) at% of NG-300, NG-500, NG-700, and NG-800 are 4.02, 5.7, 4.48, and 5.22 at%, respectively. As summarized in Table 1, the N-doping levels in RGO are in the range of 4–6%, which is dependent on annealing temperature. The NG-500 has the highest N content of

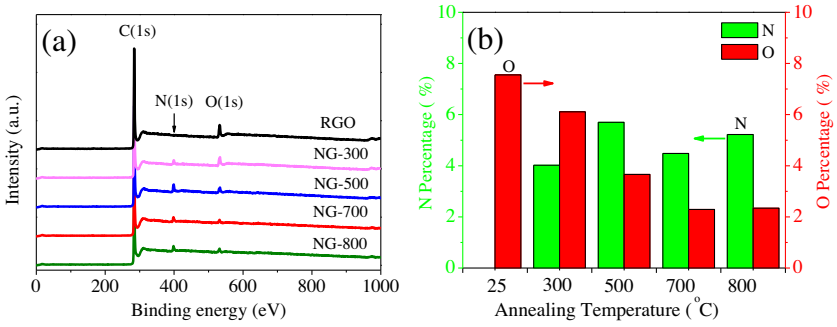

Fig. 3 – (a) XPS spectra of the RGO and NG samples obtained at different annealing temperatures. (b) Percentage of nitrogen and oxygen in the NG samples.

Table 1 – The contents of N, N-6, N-5, and N-Q in the NG samples obtained at different annealing temperatures.

NG samples (at.%)	NG-300	NG-500	NG-700	NG-800
N content	4.02	5.7	4.48	5.22
N-6 content	1.62	3.05	2.39	2.64
N-5 content	1.81	1.91	1.23	1.63
N-Q content	0.59	0.74	0.86	0.95

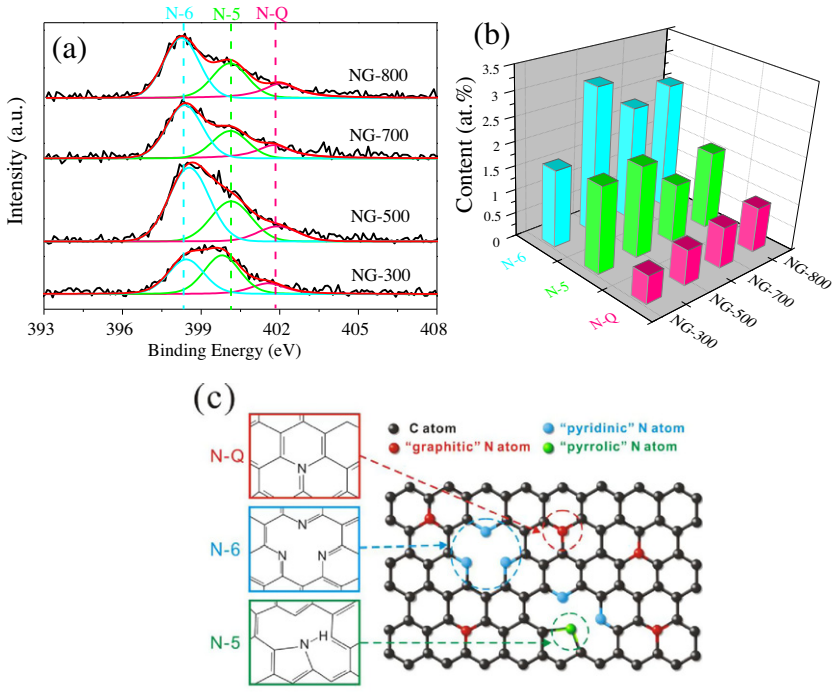

Fig. 4 – XPS spectra of the NG samples obtained at different annealing temperatures: (a) fine-scanned N 1s spectra. (b) The distributions of the three N types. (c) Schematic representation of NG.

5.7%, and NG-300 has the lowest one of 4.02% (Fig. 3(b)). Moreover, one can find that the atomic percentage of oxygen is reduced from 7.55% for RGO to 2.29% for NG-700, indicating that some oxygen-containing functional groups were removed during annealing. This is due to the formation of C–N bonds and reduction effects of thermal annealing in ammonia [26].

To get information on the incorporation of nitrogen into carbon, the N 1s spectra were fine-scanned (shown in Fig. 4(a)). Shown in Fig. 4(a) are the N 1s spectra and the fitted curves. The N 1s peaks of the NG samples were obtained and each peak was deconvoluted into three subpeaks at 398.3, 400.1, and 401.8 eV. As illustrated in Fig. 4(c), the peaks at 398.3 and 400.1 eV can be assigned to pyridine-like (N-6) and pyrrole-like (N-5), respectively. They refer to the N atoms which contribute to the π system with one or two p-electrons [27,28]. The peak at 401.8 eV corresponds to graphite-like (N-Q), implying that the N atoms replace C atoms in the RGO layers [28]. The portions of each N-configuration after annealing are graphically summarized in Fig. 4(b). Based on XPS results, the content of the N species at different annealing temperatures was quantitatively showed in Table 1. One can see that N-doping takes place at basal planes and edges, which is different from previous reports [13,29] that N-doping would take place only at edges due to the higher reactivities. Moreover, with the increasing of annealing temperature (i) the N-Q portion continuously increases; (ii) the N-6 portion increases significantly from 300 to 500 °C, then quickly decreases above 500 °C, and (iii) the N-5 portion remains relatively steady. It is clear that NG samples have been successfully synthesized by annealing RGO in an ammonia atmosphere.

To explore the optical properties of the RGO and NG samples, PL study was performed. Shown in Fig. 5(a) are the PL spectra of the RGO and NG samples with an excitation wavelength of 220 nm. For RGO, a clear emission peak at *ca*. 367 nm with a full width at half maximum of *ca*. 22 nm can be clearly observed. The strong UV emission is consistent with that observed by Shukla et al., which is attributed to the effects of quantum confinement in RGO [30]. Interestingly, one can find that (i) the NG samples exhibit a dramatic decreasing in the intensities compared to the RGO; (ii) the decreasing in the NG-500 is more apparent than other NG samples. Apparently, doping RGO with N can result in fluorescence quenching, which may attribute to the effective charge transfer between N and RGO as reported by Schedin et al. [31].

Additionally, the PL spectra of most carbon materials are dependent on excitation wavelength. However, the NG samples exhibit an excitation-independent PL behavior. The peak

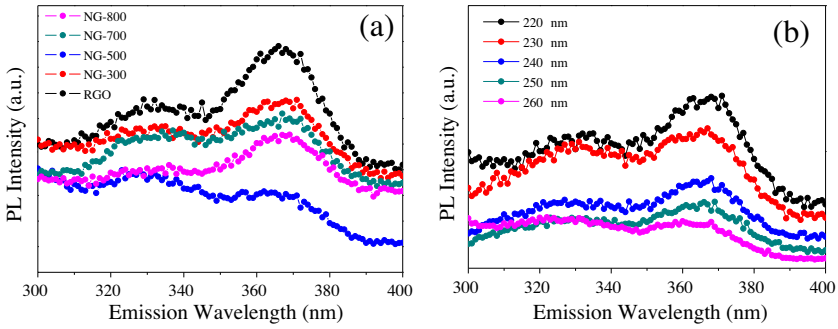

Fig. 5 – (a) PL spectra of the RGO and NG samples with excitation wavelength 220 nm. (b) PL spectra of NG-300 with different excitation wavelength from 220 to 260 nm.

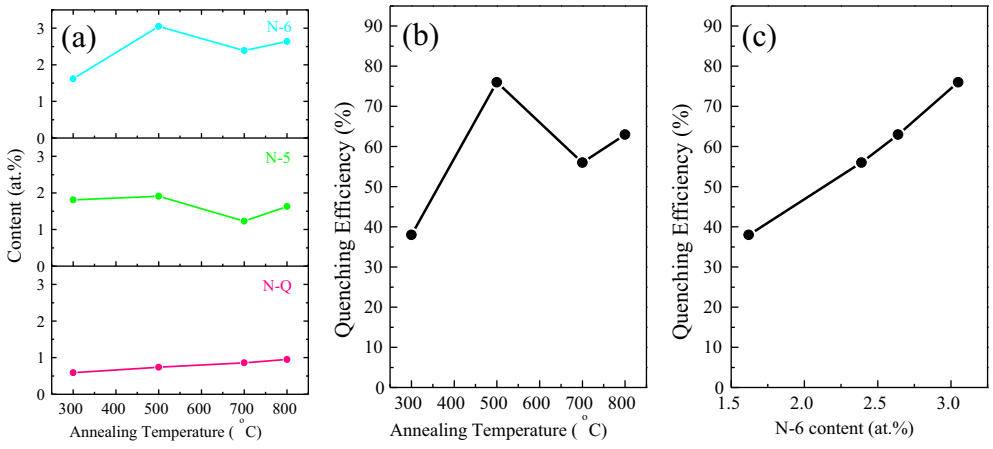

Fig. 6 – (a) The distributions of the three N types for the NG samples obtained at different annealing temperatures. (b) The dependence of the quenching efficiency on annealing temperature. (c) The dependence of the quenching efficiency on N-6 content.

positions are almost invariable at *ca*. 367 nm when the excitation wavelength is varied from 220 to 260 nm. Shown in Fig. 5(b) is a typical example of excitation-independent PL behavior. Moreover, with the excitation wavelength increasing from 220 to 260 nm, one can find that the intensity of the PL peak centered at 367 nm decreases rapidly and reaches a maximum at an excitation wavelength of 220 nm.

Fig. 6(a) reveals that the distributions of the three N types for the NG samples obtained at different annealing temperatures. According to the calculations, the dependences of quenching efficiency on annealing temperature and N-6 content are shown in Fig. 6(b) and (c), respectively. As shown in Fig. 6(b), quenching of the fluorescence emission is 38% for NG-300, while a much higher quenching of 76% is observed for NG-500. Interestingly, one can find that the quenching efficiency of NG samples is almost proportional to the N-6 content (shown in Fig. 6(c)). On the basis of the results, it is reasonable to conclude that (i) N-6 can result in the fluorescence quenching and (ii) the quenching efficiency can be increased greatly with the increase of N-6 content. In other words, by controlling the N-6 content, it is possible to tailor the quenching efficiency of NG samples.

The high efficiency quenching could be attributed to either energy transfer or electron transfer between N and RGO [32]. Possible pathways for the fluorescence quenching of the NG samples may be attributed to two possible competitive processes, *viz*., photoinduced electron transfer (PET) and energy transfer. Similar fluorescence quenching has been observed for the hybrids of carbon material with porphyrins, and a PET mechanism has been demonstrated for these hybrids [7,33]. Therefore, after photoexitation, the inteamolecular donor–acceptor interaction between N and RGO in the NG samples may have a charge transfer from N to RGO, resulting in the observed fluorescence quenching. Considering the efficient fluorescence quenching of NG, we believe that the photoinduce electron and/or energy transfer from N to RGO should play an important role for the quenching.

4. Conclusion

We have synthesized NG samples by annealing RGO in an ammonia atmosphere. The study showed that RGO has UV PL at 367 nm. The PL can be quenched by doping with N, and the fluorescence quenching efficiency is closely related to the pyridine N of NG samples. Thus, we have illustrated how the nitrogen doping content and type, and fluorescence quenching efficiency of NG samples can be manipulated. By selecting an annealing temperature, one can tailor fluorescence quenching efficiency by tuning pyridine nitrogen content of NG samples.

Acknowledgements

This work was financially supported by the State Key Program for Basic Research (Grant Nos. 2012CB932304 and 2010CB923402), NSFC (Grant No. 51072079), and the Scientific Research Foundation of Graduate School of Nanjing University (Grant No. 2012cl05) of China.

REFERENCES

[1] Novoselov KS, Geim AK, Morozov SV, Jiang D, Zhang Y, Dubonos SV, et al. Electric field effect in atomically thin carbon films. Science 2004;306:666–9.
[2] Wang J, Hernandez Y, Lotya M, Coleman JN, Blau WJ. Broadband nonlinear optical response of graphene dispersions. Adv Mater 2009;21:2430–5.
[3] Liu ZB, Wang Y, Zhang XL, Xu YF, Chen YS, Tian JG. Nonlinear optical properties of graphene oxide in nanosecond and picosecond regimes. Appl Phys Lett 2009;94:021902.
[4] Lu CH, Yang HH, Zhu CL, Chen X, Chen GN. A graphene platform for sensing biomolecules. Angew Chem Int Ed 2009;48:4785–7.
[5] Xie LM, Ling X, Fang Y, Zhang J, Liu ZF. Graphene as a substrate to suppress fluorescence in resonance Raman spectroscopy. J Am Chem Soc 2009;131:9890–1.
[6] Treossi E, Melucci M, Liscio A, Gazzano M, Samori P, Palermo V. High-contrast visualization of graphene oxide on dye-sensitized glass, quartz, and silicon by fluorescence quenching. J Am Chem Soc 2009;131:15576–7.
[7] Xu YF, Liu ZB, Zhang XL, Wang Y, Tian JG, Huang Y, et al. A graphene hybrid material covalently functionalized with porphyrin: synthesis and optical limiting property. Adv Mater 2009;21:1275–9.
[8] Xu YX, Zhao L, Bai H, Hong WJ, Li C, Shi GQ. Chemically converted graphene induced molecular flattening of 5,10,15,20-tetrakis(1-methyl-4-pyridinio)porphyrin and its application for optical detection of cadmium(II) ions. J Am Chem Soc 2009;131:13490–7.
[9] Matte HSSR, Subrahmanyam KS, Rao KV, George SJ, Rao CNR. Quenching of fluorescence of aromatic molecules by graphene due to electron transfer. Chem Phys Lett 2011;506:260–4.
[10] Bi S, Zhao TT, Luo BY. A graphene oxide platform for the assay of biomolecules based on chemiluminescence resonance energy transfer. Chem Commun 2012;48(1):106–8.
[11] Swathi RS, Sebastian KL. Resonance energy transfer from a dye molecule to graphene. J Chem Phys 2008;129:054703.
[12] Swathi RS, Sebastian KL. Long range resonance energy transfer from a dye molecule to graphene has (distance)(-4) dependence. J Chem Phys 2009;130:086101.
[13] Wang XR, Li XL, Zhang L, Yoon YK, Weber PK, Wang HL, et al. N-doping of graphene through electrothermal reactions with ammonia. Science 2009;324:768–71.
[14] Wei DC, Liu YQ, Wang Y, Zhang HL, Huang LP, Yu G. Synthesis of N-doped graphene by chemical vapor deposition and its electrical properties. Nano Lett 2009;9:1752–8.
[15] Cervantes-Sodi F, Csányi G, Piscanec S, Ferrari A. Edge-functionalized and substitutionally doped graphene nanoribbons: Electronic and spin properties. Phys Rev B 2008;77:165427.
[16] Deifallah M, McMillan PF, Cora F. Electronic and structural properties of two-dimensional carbon nitride graphenes. J Phys Chem C 2008;112(14):5447–53.
[17] Wu ZS, Ren WC, Gao LB, Liu BL, Jiang CB, Cheng HM. Synthesis of high-quality graphene with a pre-determined number of layers. Carbon 2009;47:493–9.
[18] Li M, Tang NJ, Ren WC, Cheng HM, Wu WB, Zhong W, et al. Quenching of fluorescence of reduced graphene oxide by nitrogen-doping. Appl Phys Lett 2012;100:233112.
[19] Soin N, Sinha Roy S, Roy S, Hazra KS, Misra DS, Lim TH, et al. Enhanced and stable field emission from in situ nitrogen-doped few-layered graphene nanoflakes. J Phys Chem C 2011;115:5366–72.

[20] Kudin KN, Ozbas B, Schniepp HC, Prud'homme RK, Aksay IA, Car R. Raman spectra of graphite oxide and functionalized graphene sheets. Nano Lett 2008;8:36–41.
[21] Wu ZS, Ren WC, Gao LB, Zhao JP, Chen ZP, Liu BL, et al. Synthesis of graphene sheets with high electrical conductivity and good thermal stability by hydrogen arc discharge exfoliation. ACS Nano 2009;3:411–7.
[22] Guo BD, Liu Q, Chen ED, Zhu HW, Fang L, Gong JR. Controllable N-doping of graphene. Nano Lett 2010;10:4975–80.
[23] Deng DH, Pan XL, Yu L, Cui Y, Jiang YP, Qi J, et al. Toward N-doped graphene via solvothermal synthesis. Chem Mater 2011;23:1188–93.
[24] Lin YC, Lin CY, Chiu PW. Controllable graphene N-doping with ammonia plasma. Appl Phys Lett 2010;96:133110.
[25] Cancado LG, Takai K, Enoki T, Endo M, Kim YA, Mizusaki H, et al. General equation for the determination of the crystallite size La of nanographite by Raman spectroscopy. Appl Phys Lett 2006;88:163106.
[26] Li XL, Wang HL, Robinson JT, Sanchez H, Diankov G, Dai HJ. Simultaneous nitrogen doping and reduction of graphene oxide. J Am Chem Soc 2009;131:15939–44.
[27] Wang XB, Liu YQ, Zhu DB, Zhang L, Ma HZ, Yao N, et al. Controllable growth, structure, and low field emission of well-aligned CNx nanotubes. J Phys Chem B 2002;106:2186–90.
[28] Casanovas J, Ricart JM, Rubio J, Illas F, Jimenez-Mateos JM. Origin of the large N is binding energy in X-ray photoelectron spectra of calcined carbonaceous materials. J Am Chem Soc 1996;118:8071–6.
[29] Wang XR, Tabakman SM, Dai HJ. Atomic layer deposition of metal oxides on pristine and functionalized graphene. J Am Chem Soc 2008;130:8152–3.
[30] Shukla S, Saxena S. Spectroscopic investigation of confinement effects on optical properties of graphene oxide. Appl Phys Lett 2011;98:073104.
[31] Schedin F, Geim AK, Morozov SV, Hill EW, Blake P, Katsnelson MI, et al. Detection of individual gas molecules adsorbed on graphene. Nat Mater 2007;6:652–5.
[32] He SJ, Song B, Li D, Zhu CF, Qi WP, Wen YQ, et al. A graphene nanoprobe for rapid, sensitive, and multicolor fluorescent DNA analysis. Adv Funct Mater 2010;20:453–9.
[33] Baskaran D, Mays JW, Zhang XP, Bratcher MS. Carbon nanotubes with covalently linked porphyrin antennae: photoinduced electron transfer. J Am Chem Soc 2005;127:6916–7.